Supplementary information

TABLE OF CONTENTS

*Figure S1. Typical DMPO-CH_3 signal [15] (a) and DMPO-COO^- signal (simulated based on constants given by Mossoba et al. [26]) (b) - DMPO-CH_3: a_H=16.1 G, a_N=23.0 G; DMPO-COO^-: a_H=15.6 G, a_N=18.7 G ..... **Error! Bookmark not defined.***

Table S1. DMPO+Cu-Phen – Simulation results 4

Figure S2. Comparison between the experimental and simulated spectra of DMPO+Cu-Phen 4

Table S2. DMPO+Cu-Phen+H_2O_2 – Simulation results 5

Figure S3. Comparison between the experimental and simulated spectra of DMPO+Cu-Phen+H_2O_2 at near-neutral pH 5

Table S3. DMSO+DMPO+Cu-Phen+H_2O_2 – Simulation results 6

Figure S4. Comparison between the experimental and simulated spectra of DMSO+DMPO+Cu-Phen+H_2O_2 6

Table S4. $HCOO^-$+DMPO+Cu-Phen+H_2O_2 – Simulation results 6

Figure S5. Comparison between the experimental and simulated spectra of $HCOO^-$+DMPO+Cu-Phen+H_2O_2 7

Table S5. DMPO+$CuSO_4$ – Simulation results 7

Table S6. $HCOO^-$+DMPO+Cu-Phen+H_2O_2 t=5 min – Simulation results 7

Table S7. $HCOO^-$+DMPO+Cu-Phen+H_2O_2 after heating – Simulation results 7

Table S8. DMPO+$CuSO_4$+H_2O_2 – Simulation results 8

Table S9. DMSO+DMPO+$CuSO_4$+H_2O_2 – Simulation results 8

Table S10. $HCOO^-$+DMPO+$CuSO_4$+H_2O_2 – Simulation results 8

Table S11. DMPO+$FeSO_4$+H_2O_2 at pH 3 – Simulation results 8

Table S12. DMSO+DMPO+$CuSO_4$ – Simulation results 9

Table S13. DMSO+DMPO+Cu-Phen – Simulation results 9

Table S14. $HCOO^-$+DMPO+Cu-Phen – Simulation results 9

Table S15. $HCOO^-$+DMPO+Cu-Phen after heating – Simulation results 9

Table S16. DMPO+H_2O_2 after heating – Simulation results 10

Table S17. NaOH+DMPO+$CuSO_4$ – Simulation results 10

Table S18. NaOH+DMPO+Cu-Phen – Simulation results 10

Table S19. NaOH+$HCOO^-$+DMPO+Cu-Phen t=8 min – Simulation results 10

Table S20. NaOH+DMPO+Cu-Phen+H_2O_2 – Simulation results 11

Table S21. NaOH+DMSO+DMPO+Cu-Phen+H_2O_2 – Simulation results 11

Table S22. NaOH+$HCOO^-$+DMPO+Cu-Phen+H_2O_2 – Simulation results 11

Figure S6. X-band EPR spectra of DMPO+Cu-Phen and $HCOO^-$+DMPO+Cu-Phen - The simulation revealed the presence of four radical species with $HCOO^-$+DMPO+Cu-Phen: DMPO-OH, a_N = 14.843 G, a_H = 15.428 G; DMPO-R, a_N = 15.644 G, a_H = 23.244 G; triplet, a_N = 14.593 G; DMPO-COO^-, a_N = 15.683 G, a_H = 19.293 G - Assignments: o=DMPO-OH, |=DMPO-R, +=triplet, |=DMPO-COO^- 12

Figure S7. X-band EPR spectra of DMPO+Cu-Phen and $HCOO^-$+DMPO+Cu-Phen after heating – The simulation revealed the presence of four radical species with $HCOO^-$+DMPO+Cu-Phen: DMPO-OH, a_N = 14.746 G, a_H = 15.428 G; DMPO-R, a_N = 15.644 G, a_H = 23.342 G; triplet, a_N = 14.788 G; DMPO-COO^-, a_N = 15.781 G, a_H = 19.0 G - Assignments: o=DMPO-OH, |=DMPO-R, +=triplet, |=DMPO-COO^- 13

Figure S8. X-band EPR spectra of DMPO+H_2O_2 at ambient temperature and after heating. The simulation revealed the presence of three radical species after heating: DMPO-OH, a_N = 14.756 G, a_H = 15.391 G; DMPO-R, a_N = 14.813 G, a_H = 21.535 G; triplet, a_N = 14.842 G - Assignments: o=DMPO-OH, |=DMPO-R, +=triplet 13

Figure S9. X-band EPR spectra of DMPO+Cu-Phen+H_2O_2 and $HCOO^-$+DMPO+Cu-Phen+H_2O_2 - With $HCOO^-$, the simulation revealed the presence of four radical species DMPO-OH, a_N = 14.902 G, a_H = 15.233 G; DMPO-R, a_N = 15.64 G, a_H = 23.266 G; triplet, a_N = 14.593 G; DMPO-COO^-, a_N = 15.749 G, a_H = 19.098 G - Assignments: o=DMPO-OH, |=DMPO-R, +=triplet, |=DMPO-COO^- 14

Figure S10. X-band EPR spectra of $HCOO^-$+DMPO+Cu-Phen+H_2O_2 at ambient temperature at t=0 and t=10 min and after heating - The simulations revealed the presence of four radical species. At t=10 min: DMPO-OH, a_N = 15.049 G, a_H = 14.976 G; DMPO-R, a_N = 15.651 G, a_H = 23.872 G; triplet, a_N = 14.463 G; DMPO-COO^-, a_N = 15.781

G, a_H = 19.098 G [26], [32]. After heating: DMPO-OH, a_N = 15.0 G, a_H = 15.074G; DMPO-R, a_N = 15.602 G, a_H = 23.607 G; triplet, a_N = 14.512 G; DMPO-COO^-, a_N = 15.781 G, a_H = 19.049 G - Assignments: |=DMPO-COO^-.....15
Figure S11. X-band EPR spectra of NaOH+DMPO and NaOH+DMPO+Phen - Assignments: +=triplet.....16
Figure S12. X-band EPR spectra of NaOH+DMPO+$CuSO_4$ and NaOH+DMPO+Cu-Phen - The simulations revealed the presence of four radical species in both solutions. With $CuSO_4$: DMPO-OH, a_N = 15.195 G, a_H = 15.294 G; DMPO-R, a_N = 15.741 G, a_H = 23.488 G; triplet, a_N = 14.549 G; other, a_H = 17.975 G (2 H, uncertain). With Cu-Phen: DMPO-OH, a_N = 15.234 G, a_H = 15.623 G; DMPO-R, a_N = 15.742 G, a_H = 23.83 G; triplet, a_N = 14.398 G; other, a_N = 14.999 G, a_H = 21.246 G - Assignments: o=DMPO-OH, |=DMPO-R, +=triplet.....16
Figure S13. X-band EPR spectra of NaOH+$HCOO^-$+DMPO+Cu-Phen at t=0, t=5 min and t=8 min - The simulations revealed the presence of two radical species: DMPO-R, a_N = 15.595 G, a_H = 22.756 G; DMPO-COO^-, a_N = 15.805 G, a_H = 19.00 G.....17
Figure S14. X-band EPR spectra at 100 K of (a) NaOH+Cu-Phen with and without DMPO - [Cu] = 0.15 mM, [DMPO] = 60 mM, and (b) NaOH+$CuSO_4$ with and without DMPO - [DMPO] = 60 mM. The addition of DMPO at the same concentration as Cu-Phen (0.15 mM) did not seem to modify the structure of Cu(II) (not shown). 17
Figure S15. X-band EPR spectra of NaOH+DMPO+Cu-Phen+H_2O_2 at t=0 and at t=5 min - Assignments: o=DMPO-OH.....18
Figure S16. X-band EPR spectra of NaOH+DMPO+$CuSO_4$ and NaOH+DMPO+$CuSO_4$+H_2O_2.....18
Table S23. EPR hyperfine coupling constants of the observed radical species: experimental and reference values (see Buettner's spin adduct parameter tables [13]) for comparison 19
Table S24. Simulation results for the EPR spectra recorded at 100 K: EPR parameters given as g-values and A-values for each experimental spectrum.....20
Figure S17. X-band EPR spectrum at 100 K of CuSO4 and corresponding simulated spectrum 20
Figure S18. X-band EPR spectrum at 100 K of DMPO+CuSO4 and corresponding simulated spectrum 21
Figure S19. X-band EPR spectrum at 100 K of Cu-Phen and corresponding simulated spectrum 21
Figure S20. X-band EPR spectrum at 100 K of DMPO+Cu-Phen and corresponding simulated spectrum.....22
Figure S21. X-band EPR spectrum at 100 K of NaOH+CuSO4 and corresponding simulated spectrum 22
Figure S22. X-band EPR spectrum at 100 K of NaOH+DMPO+CuSO4 and corresponding simulated spectrum 23
Figure S23. X-band EPR spectrum at 100 K of NaOH+ Cu-Phen and corresponding simulated spectrum 23
Figure S24. X-band EPR spectrum at 100 K of NaOH+DMPO+Cu-Phen and corresponding simulated spectrum....24

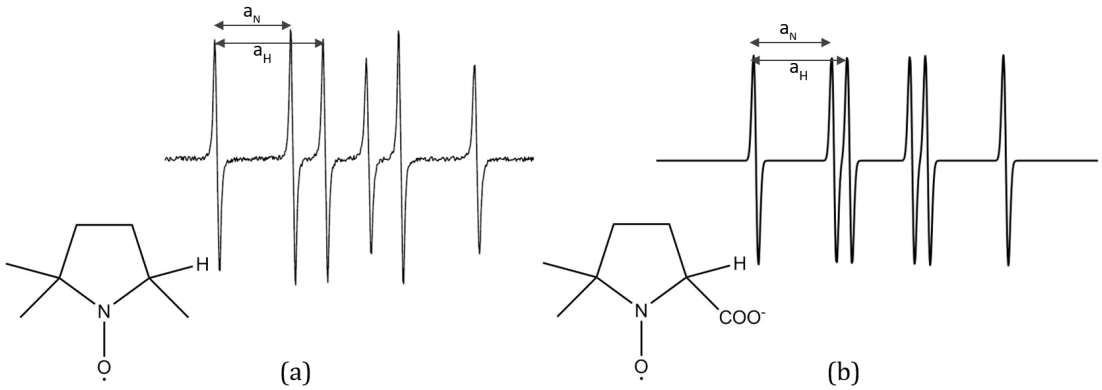

Figure S1. Typical DMPO-CH_3 signal [15] (a) and DMPO-COO^- signal (simulated based on constants given by Mossoba et al. [26]) (b) - DMPO-CH_3: a_H=16.1 G, a_N=23.0 G; DMPO-COO^-: a_H=15.6 G, a_N=18.7 G

The supplementary material presented below illustrates the EPR simulations performed to find the relative amounts of different DMPO adducts during the spin-trapping experiments.

The details of the simulation results for DMPO+Cu-Phen are given in Table S1 and the simulated spectrum is compared to the experimental spectrum in Figure S2. Similar Tables and Figures are given for DMPO+Cu-Phen+H_2O_2 (Table S2 and Figure S3), DMSO+DMPO+Cu-Phen+H_2O_2 (Table S3 and Figure S4), and $HCOO^-$+DMPO+Cu-Phen+H_2O_2 (Table S4 and Figure S5). Table S5 to Table S22 show all the other simulation results from recorded EPR spectra.

Table S1. DMPO+Cu-Phen (exp 2) – Simulation results

	DMPO-OH	DMPO-R	Triplet
a_N (G)	15.088	15.781	14.354
a_H (G)	14.943	23.27	/
L_w (G)	0.500/0.449/0.458	0.902/0.846/0.952	0.756/0.756/0.805
Lorentzian (%)		18	
Relative area (%)	6	77	17

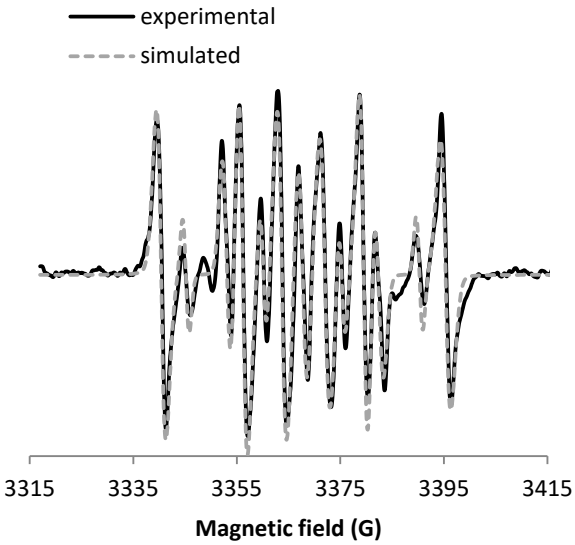

Figure S2. Comparison between the experimental and simulated spectra of DMPO+Cu-Phen (exp 2)

Table S2. DMPO+Cu-Phen+H_2O_2 (exp 3) – Simulation results

	DMPO-OH	DMPO-R	Triplet
a_N (G)	15	15.781	14.549
a_H (G)	14.805	23.342	/
L_w (G)	0.609/0.658/0.609	0.988/0.988/1.049	0.854/0.805/0.854
Relative area (%)	38	53	8

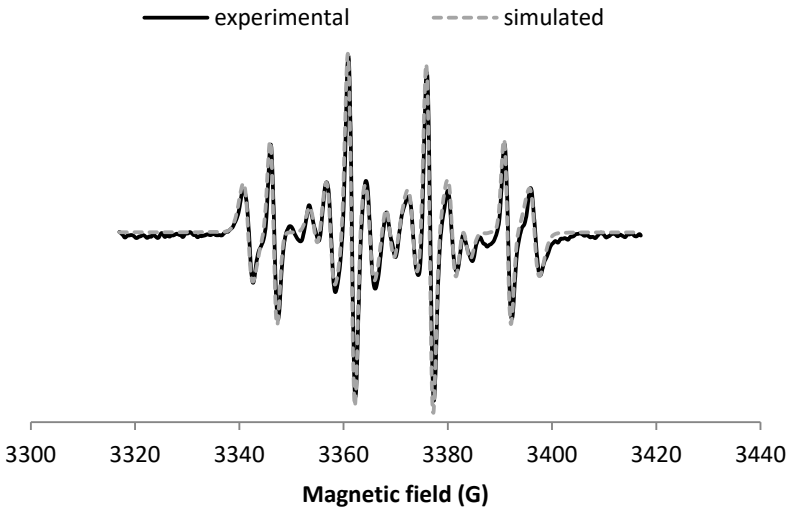

Figure S3. Comparison between the experimental and simulated spectra of DMPO+Cu-Phen+H_2O_2 (exp 3) at near-neutral pH

Table S3. DMSO+DMPO+Cu-Phen+H_2O_2 (exp 4) – Simulation results

	DMPO-OH	DMPO-CH_3	Triplet	DMPO-R
a_N (G)	14.7	15.7	14.349	15.786
a_H (G)	13.851	22.651	/	20.11
L_w (G)	0.658/0.659/0.658	1.086/0.951/1.098	0.805/0.756/0.854	0.852/0.754/1.974
relative area (%)	18	73	5	5

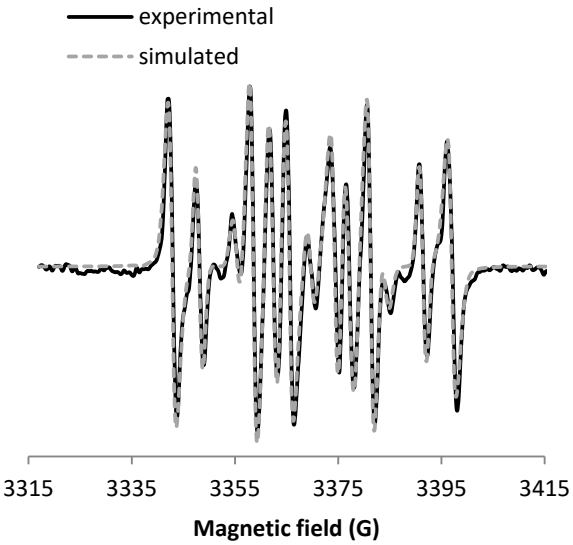

Figure S4. Comparison between the experimental and simulated spectra of DMSO+DMPO+Cu-Phen+H_2O_2 (exp 4)

Table S4. $HCOO^-$+DMPO+Cu-Phen+H_2O_2 (exp 5) – Simulation results

	DMPO-OH	DMPO-R	Triplet	DMPO-COO^-
a_N (G)	14.902	15.64	14.593	15.749
a_H (G)	15.233	23.266	/	19.098
L_w (G)	0.649/0.561/0.609	1.047/1.047/1.193	0.708/0.708/0.898	0.551/0.551/0.551
Relative area (%)	18	28	5	49

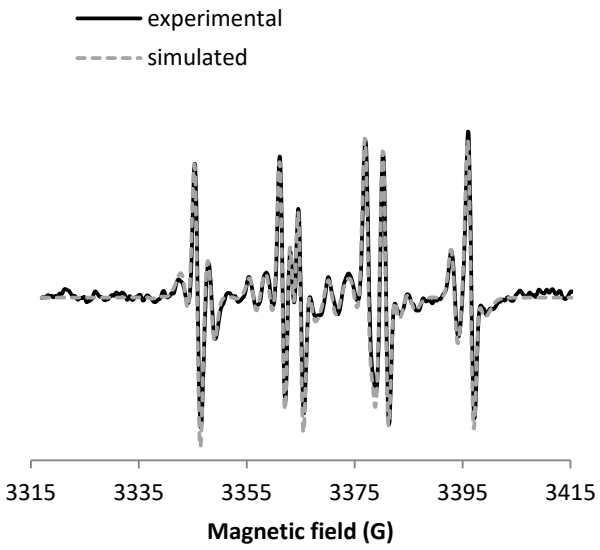

Figure S5. Comparison between the experimental and simulated spectra of $HCOO^-$+DMPO+Cu-Phen+H_2O_2 (exp 5)

Table S5. DMPO+$CuSO_4$ (exp 1) – Simulation results

	DMPO-OH	DMPO-R	Triplet	Other
a_N (G)	15.19	15.798	14.609	16.323
a_H (G)	14.928	23.237		26.653
L_w (G)	0.6/0.659/0.658	1/1.049/1.098	0.702/0.654/0.751	1.291/2.463/1.632
Relative area (%)	5	74	8	13

Table S6. $HCOO^-$+DMPO+Cu-Phen+H_2O_2 t=5 min (exp 5) – Simulation results

	DMPO-OH	DMPO-R	Triplet	DMPO-COO^-
a_N (G)	15.049	15.651	14.463	15.781
a_H (G)	14.976	23.872		19.098
L_w (G)	0.649/0.610/0.658	1/1/1.098	0.897/1.191/1.093	0.6/0.6/0.6
Relative area (%)	14	12	4	70

Table S7. $HCOO^-$+DMPO+Cu-Phen+H_2O_2 after heating (exp 7) – Simulation results

	DMPO-OH	DMPO-R	Triplet	DMPO-COO^-
a_N (G)	15	15.602	14.512	15.781
a_H (G)	15.074	23.607		19.049
L_w (G)	0.649/0.561/0.6	0.902/0.805/0.951	0.854/0.854/1.049	0.551/0.551/0.551
Relative area (%)	10	8	3	79

Table S8. DMPO+$CuSO_4$+H_2O_2 (exp 8) – Simulation results

	DMPO-OH	DMPO-R	Triplet	Other	Other
a_N (G)	15.244	15.7	14.598	13.975	12.195
a_H (G)	14.83	23.51		21.435	11.463 (3H)
L_w (G)	0.6/0.561/0.649	1.049/1.049/1.195	0.805/0.903/0.951	1/0.805/1.488	0.751/6.855/0.898
Relative area (%)	7	57	16	10	9

Table S9. DMSO+DMPO+$CuSO_4$+H_2O_2 (exp 9) – Simulation results

	DMPO-OH	DMPO-R	Triplet
a_N (G)	14.707	15.651	14.354
a_H (G)	13.951	22.658	
L_w (G)	0.651/0.708/0.697	1/1.049/1.244	0.756/0.756/0.805
Relative area (%)	16	76	8

Table S10. $HCOO^-$+DMPO+$CuSO_4$+H_2O_2 (exp 10) – Simulation results

	DMPO-OH	DMPO-R	Triplet	DMPO-COO^-	Other
a_N (G)	15.269	15.749	14.695	15.793	13.709
a_H (G)	14.951	23.559		18.97	7.508 (3H)
L_w (G)	0.651/0.561/0.648	1.244/1.1049/1.293	0.805/0.854/0.951	0.556/0.556/0.556	1.288/1.484/1.142
Relative area (%)	15	34	10	23	18

Table S11. DMPO+$FeSO_4$+H_2O_2 at pH 3 (exp 11) – Simulation results

	DMPO-OH	DMPO-R	Triplet
a_N (G)	15	14.675	14.793
a_H (G)	14.732	21.703	
L_w (G)	0.651/0.708/0.697	1/1.098/1.586	0.952/0.854/0.854
Relative area (%)	86	7	7

Table S12. DMSO+DMPO+$CuSO_4$ (exp 12) – Simulation results

	DMPO-OH	DMPO-R	Triplet
a_N (G)	14.697	15.439	14.354
a_H (G)	14.015	22.586	
L_w (G)	0.597/0.644/0.644	1/0.944/1.049	0.707/0.658/0.756
Lorentzian (%)		85	
Relative area (%)	14	78	8

Table S13. DMSO+DMPO+Cu-Phen (exp 13) – Simulation results

	DMPO-OH	DMPO-R	Triplet
a_N (G)	14.697	15.488	14.305
a_H (G)	13.82	22.635	
L_w (G)	0.597/0.595/0.595	1/0.944/1.049	0.707/0.658/0.756
Lorentzian (%)		76	
Relative area (%)	22	72	6

Table S14. $HCOO^-$+DMPO+Cu-Phen (exp 14) – Simulation results

	DMPO-OH	DMPO-R	DMPO-COO^-	Triplet
a_N (G)	14.843	15.644	15.683	14.593
a_H (G)	15.428	23.244	19.293	
L_w (G)	0.499/0.4/0.498	0.902/0.902/1.000	0.463/0.651/0.500	0.756/0.756/0.854
Lorentzian (%)		42	98	
Relative area (%)	19	58	11	12

Table S15. $HCOO^-$+DMPO+Cu-Phen after heating (exp 15) – Simulation results

	DMPO-OH	DMPO-R	DMPO-COO^-	Triplet
a_N (G)	14.746	15.644	15.781	14.788
a_H (G)	15.428	23.342	19	
L_w (G)	0.548/0.302/0.546	0.902/0.902/1.098	0.463/0.546/0.463	0.805/0.756/1.195
Lorentzian (%)			28	
Relative area (%)	11	13	72	4

Table S16. DMPO+H_2O_2 after heating (exp 16) – Simulation results

	DMPO-OH	DMPO-R	Triplet
a_N (G)	14.756	14.813	14.842
a_H (G)	15.391	21.535	
L_w (G)	0.549/0.451/0.500	1.045/2/1.830	0.903/0.893/0.996
Lorentzian (%)	36	42	9
Relative area (%)	38	38	24

Table S17. NaOH+DMPO+$CuSO_4$ (exp 17) – Simulation results

	DMPO-OH	DMPO-R	Triplet	Other
a_N (G)	15.195	15.741	14.549	
a_H (G)	15.294	23.488		17.975 (2H)
L_w (G)	0.402/0.402/0.305	0.800/0.995/1.288	0.610/0.800/0.654	3.3/0.7/9.6
Lorentzian (%)	8	76		
Relative area (%)	2	72	6	20

Table S18. NaOH+DMPO+Cu-Phen (exp 18) – Simulation results

	DMPO-OH	DMPO-R	Triplet	Other
a_N (G)	15.234	15.742	14.398	14.999
a_H (G)	15.623	23.83		21.246
L_w (G)	0.597/0.400/0.595	1/0.902/1.195	0.756/0.756/0.756	0.800/0.749/1.000
Lorentzian (%)		10		
Relative area (%)	17	58	10	14

Table S19. NaOH+$HCOO^-$+DMPO+Cu-Phen t=8 min (exp 19) – Simulation results

	DMPO-R	DMPO-COO^-
a_N (G)	15.595	15.805
a_H (G)	22.756	19
L_w (G)	0.658/0.658/0.658	0.507/0.451/0.451
Lorentzian (%)		37
Relative area (%)	8	92

Table S20. NaOH+DMPO+Cu-Phen+H_2O_2 (exp 20) – Simulation results

	DMPO-OH	DMPO-R	Triplet
a_N (G)	15.439	15.79	14.646
a_H (G)	15.049	23.488	
L_w (G)	0.5/0.5/0.549	1.049/1.146/1.293	0.659/0.751/0.800
Lorentzian (%)		33	
Relative area (%)	21	69	11

Table S21. NaOH+DMSO+DMPO+Cu-Phen+H_2O_2 (exp 21) – Simulation results

	DMPO-OH	DMPO-CH_3	Triplet
a_N (G)	13.926	15.937	14.788
a_H (G)	14.072	22.658	
L_w (G)	0.743/0.839/0.986	0.658/0.658/0.609	0.658/0.658/1.293
Lorentzian (%)	34	9	
Relative area (%)	16	80	5

Table S22. NaOH+$HCOO^-$+DMPO+Cu-Phen+H_2O_2 (exp 22) – Simulation results

	DMPO-OH	DMPO-R	DMPO-COO^-	Triplet
a_N (G)	15.342	15.742	15.805	14.691
a_H (G)	15.537	24.123	19.049	
L_w (G)	0.499/0.351/0.498	0.804/1.097/1.049	0.507/0.5/0.451	0.561/0.609/0.451
Lorentzian (%)	42		16	
Relative area (%)	17	28	47	8

The EPR spectra below support the discussion related to results at near-neutral pH (Figure S6 to Figure S10).

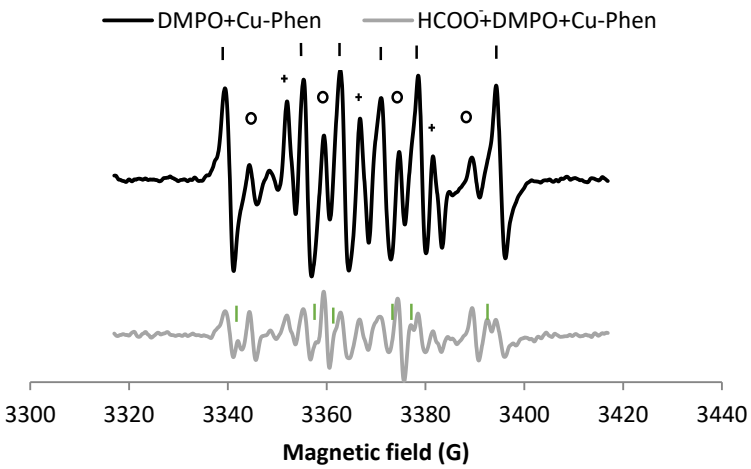

Figure S6. X-band EPR spectra of DMPO+Cu-Phen and $HCOO^-$+DMPO+Cu-Phen (exp 2 and 14) - The simulation revealed the presence of four radical species with $HCOO^-$+DMPO+Cu-Phen: DMPO-OH, a_N = 14.843 G, a_H = 15.428 G; DMPO-R, a_N = 15.644 G, a_H = 23.244 G; triplet, a_N = 14.593 G; DMPO-COO^-, a_N = 15.683 G, a_H = 19.293 G - Assignments: o=DMPO-OH, |=DMPO-R, +=triplet, |=DMPO-COO^-

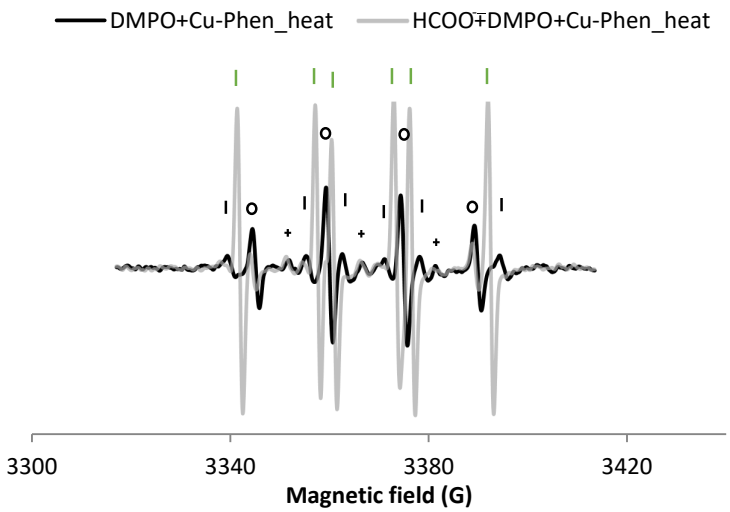

Figure S7. X-band EPR spectra of DMPO+Cu-Phen and $HCOO^-$+DMPO+Cu-Phen after heating (exp 2 and 15) – The simulation revealed the presence of four radical species with $HCOO^-$+DMPO+Cu-Phen: DMPO-OH, a_N = 14.746 G, a_H = 15.428 G; DMPO-R, a_N = 15.644 G, a_H = 23.342 G; triplet, a_N = 14.788 G; DMPO-COO^-, a_N = 15.781 G, a_H = 19.0 G - Assignments: o=DMPO-OH, |=DMPO-R, +=triplet, |=DMPO-COO^-

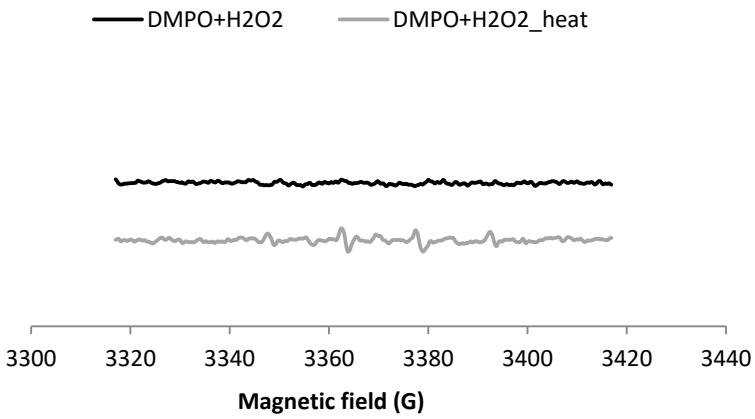

Figure S8. X-band EPR spectra of DMPO+H_2O_2 at ambient temperature and after heating (exp 16). The simulation revealed the presence of three radical species after heating: DMPO-OH, a_N = 14.756 G, a_H = 15.391 G; DMPO-R, a_N = 14.813 G, a_H = 21.535 G; triplet, a_N = 14.842 G - Assignments: o=DMPO-OH, |=DMPO-R, +=triplet

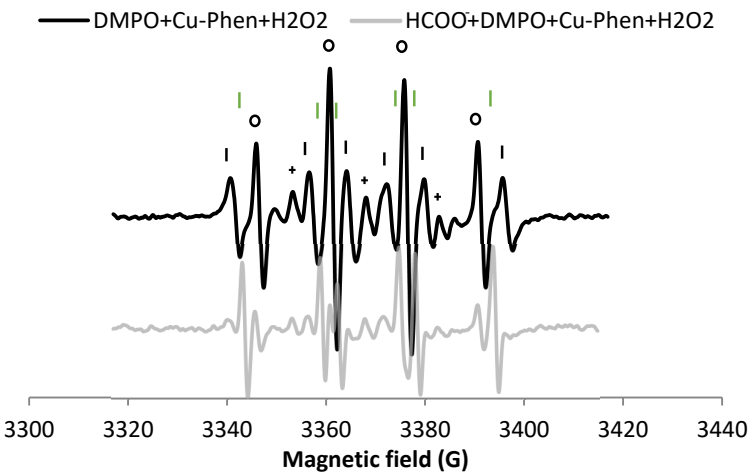

Figure S9. X-band EPR spectra of DMPO+Cu-Phen+H_2O_2 and $HCOO^-$+DMPO+Cu-Phen+H_2O_2 (exp 3 and 5) - With HCOO (exp 5), the simulation revealed the presence of four radical species DMPO-OH, a_N = 14.902 G, a_H = 15.233 G; DMPO-R, a_N = 15.64 G, a_H = 23.266 G; triplet, a_N = 14.593 G; DMPO-COO^-, a_N = 15.749 G, a_H = 19.098 G - Assignments: o=DMPO-OH, |=DMPO-R, +=triplet, |=DMPO-COO^-

DMPO-COO^- represents 49% of the detected radicals and a significant amount of DMPO-R is also found (28%) compared to the two previous solutions (without scavenger and with DMSO), suggesting stronger DMPO degradation in that case (entry 5 in Table 1).

The solution with $HCOO^-$+DMPO+Cu-Phen+H_2O_2 was also analyzed 10 min after the first acquisition (exp 6) to observe the evolution. The same experiment was repeated with heating (exp 7) to compare the intensity of radical generation.

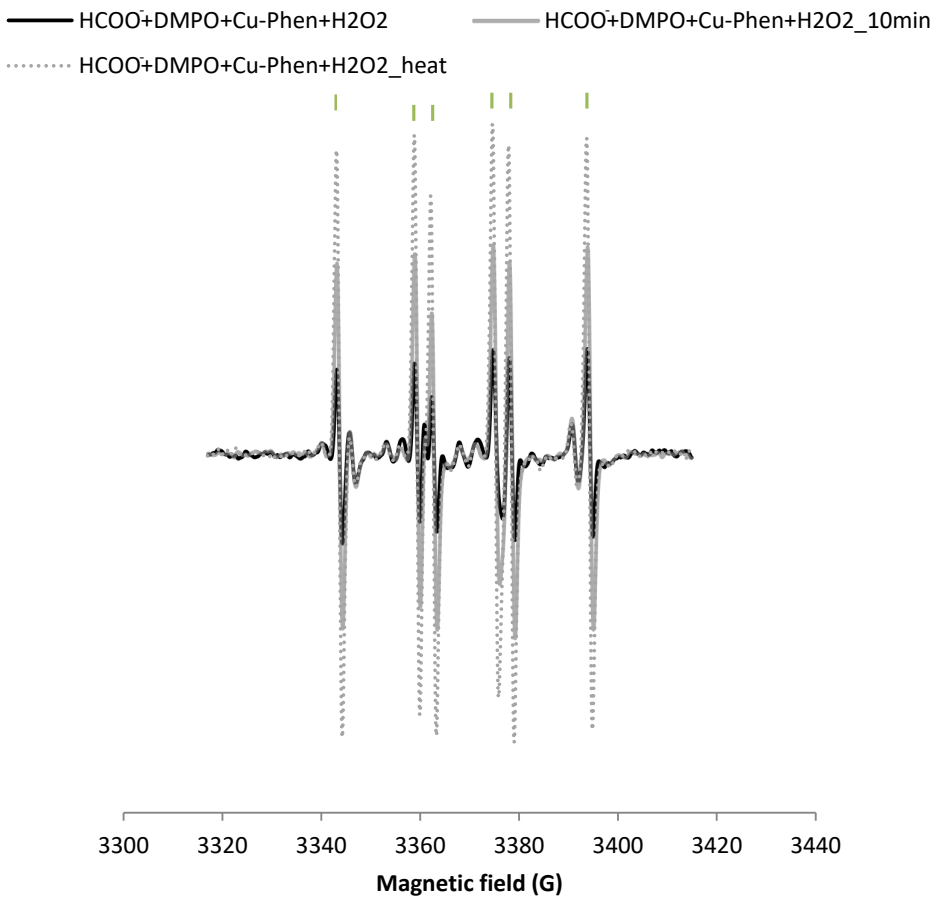

Figure S10. X-band EPR spectra of $HCOO^-$+DMPO+Cu-Phen+H_2O_2 at ambient temperature at t=0 and t=10 min and after heating - The simulations revealed the presence of four radical species. At t=10 min (exp 6): DMPO-OH, a_N = 15.049 G, a_H = 14.976 G; DMPO-R, a_N = 15.651 G, a_H = 23.872 G; triplet, a_N = 14.463 G; DMPO-COO^-, a_N = 15.781 G, a_H = 19.098 G [26], [32]. After heating (exp 7): DMPO-OH, a_N = 15.0 G, a_H = 15.074G; DMPO-R, a_N = 15.602 G, a_H = 23.607 G; triplet, a_N = 14.512 G; DMPO-COO^-, a_N = 15.781 G, a_H = 19.049 G - Assignments: |=DMPO-COO^-

After 10 min, an increase of the DMPO-COO^- signal of approximately 20% is observed (entry 6 in Table 1a; 70% DMPO-COO^- for a total peak area of 0.54 vs. 49% for a total peak area of 0.65). After heating, the signal was even stronger: 65% more intense than after 10 min at room temperature (according to the total area of 0.79 with 79% DMPO-COO^- (entry 7)).

The decomposition of DMPO at strong alkaline pH (12.3-12.5) was assessed via control experiments with DMPO alone and with phenanthroline (Figure S11).

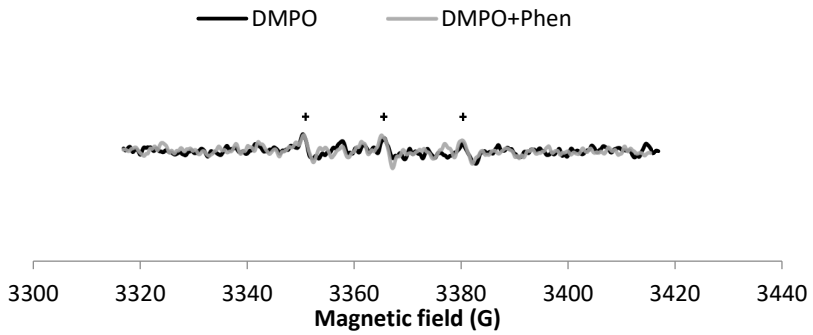

Figure S11. X-band EPR spectra of NaOH+DMPO and NaOH+DMPO+Phen - Assignments: +=triplet

DMPO alone was observed to be degraded faster than at near-neutral pH, as the same degradation 3-peak signal is observed but in the absence of copper or hydrogen peroxide. This is consistent with easier nucleophilic addition at alkaline pH. With the addition of phenanthroline, no difference was detected.

The controls with $CuSO_4$ and with Cu-Phen (exp 17 and 18) are presented in Figure S12.

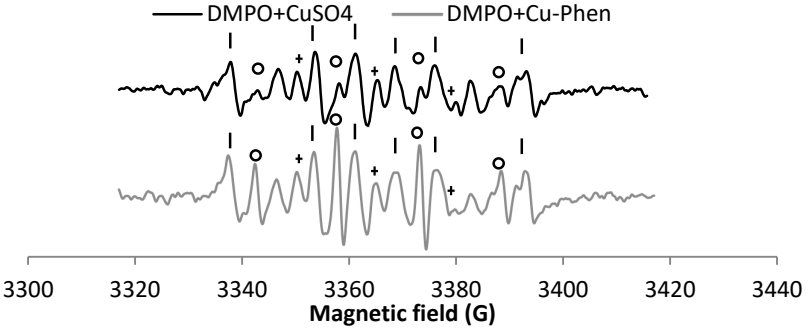

Figure S12. X-band EPR spectra of NaOH+DMPO+$CuSO_4$ and NaOH+DMPO+Cu-Phen - The simulations revealed the presence of four radical species in both solutions. With $CuSO_4$ (exp 17): DMPO-OH, a_N = 15.195 G, a_H = 15.294 G; DMPO-R, a_N = 15.741 G, a_H = 23.488 G; triplet, a_N = 14.549 G; other, a_H = 17.975 G (2 H, uncertain). With Cu-Phen (exp 18): DMPO-OH, a_N = 15.234 G, a_H = 15.623 G; DMPO-R, a_N = 15.742 G, a_H = 23.83 G; triplet, a_N = 14.398 G; other, a_N = 14.999 G, a_H = 21.246 G - Assignments: o=DMPO-OH, |=DMPO-R, +=triplet

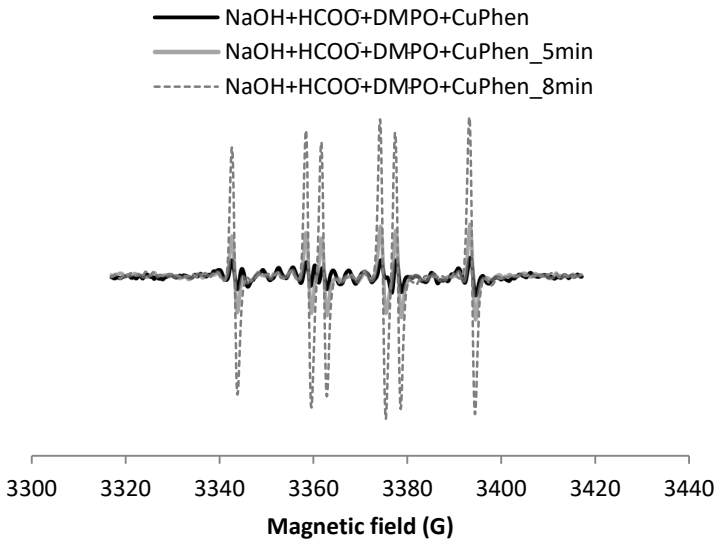

Figure S13. X-band EPR spectra of NaOH+$HCOO^-$+DMPO+Cu-Phen at t=0, t=5 min and t=8 min (exp 19) - The simulations revealed the presence of two radical species: DMPO-R, a_N = 15.595 G, a_H = 22.756 G; DMPO-COO^-, a_N = 15.805 G, a_H = 19.00 G

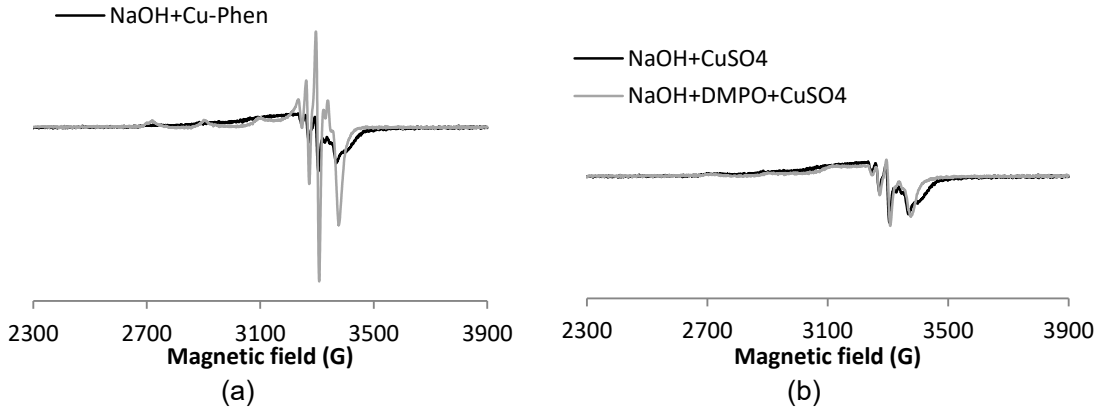

Figure S14. X-band EPR spectra at 100 K of (a) NaOH+Cu-Phen with and without DMPO - [Cu] = 0.15 mM, [DMPO] = 60 mM, and (b) NaOH+$CuSO_4$ with and without DMPO - [DMPO] = 60 mM. The addition of DMPO at the same concentration as Cu-Phen (0.15 mM) did not seem to modify the structure of Cu(II) (not shown).

When Cu-Phen was introduced at the concentration of the spin-trapping trials, i.e. 60 mM (Figure S14a), a clear hyperfine structure appeared, evidencing the interaction between Cu and DMPO. Based on the small modifications of coupling constants between the two spectra in Figure S14b, the addition of DMPO to the alkaline $CuSO_4$ solution slightly modified the structure of Cu(II).

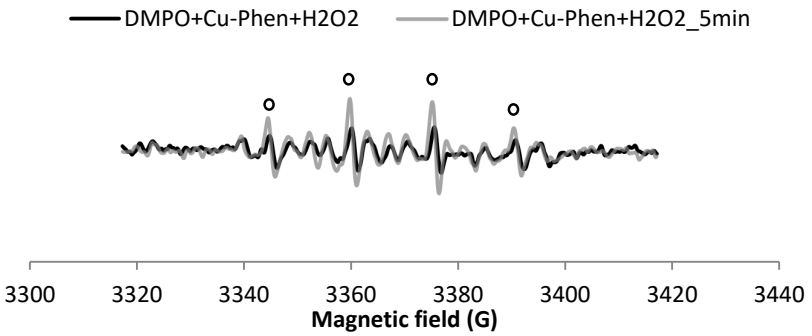

Figure S15. X-band EPR spectra of NaOH+DMPO+Cu-Phen+H_2O_2 (exp 20) at t=0 and at t=5 min - Assignments: o=DMPO-OH

The higher intensity of the DMPO-OH signal after 5 minutes illustrates the slow generation of hydroxyl radicals by the H_2O_2/Cu-Phen system under alkaline conditions.

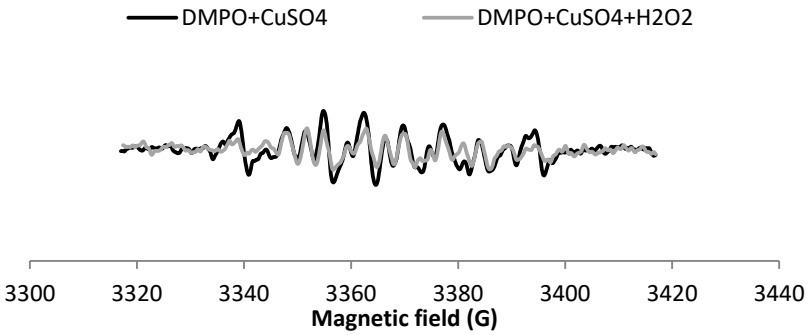

Figure S16. X-band EPR spectra of NaOH+DMPO+$CuSO_4$ (exp 17) and NaOH+DMPO+$CuSO_4$+H_2O_2

Without H_2O_2, the simulation reveals the absence of DMPO-OH (only 2% of the radical species, see Table 2, while the signal is weak). With H_2O_2, the EPR spectrum is very similar. Consequently, no hydroxyl radical production is detected.

Table S23 gathers the EPR data obtained from the present investigation in addition to selected ones of the literature to allow the assignment of the observed radical species.

Table S23. EPR hyperfine coupling constants of the observed radical species: experimental and reference values (see Buettner's spin adduct parameter tables [13]) for comparison

		DMPO triplet	DMPO-R	DMPO-OH	DMPO-CH_3	DMPO-COO^-
Number of lines (intensity)		3	6	4 (1:2:2:1)	6	6
Experimental values (from simulation)	a_{Nexp} (G)	14.3-14.8	14.8-15.8	13.9-15.4	15.4-15.9	15.7-15.8
	a_{Hexp} (G)	/	20.1-24.1	13.8-15.6	22.6-23.3	19.0-19.3
Reference values (from the literature)	a_{Nref} (G)	n/a	15.5	14.9	16.1 / 16.4	15.6
	a_{Href} (G)	/	22.0	14.9	23.0 / 23.5	18.7
	References	/	[29]	[26], [30]	[26] / [31]	[26], [32]

The following Table and Figures are supporting the results of EPR analyses performed at 100 K. Table S24 presents the simulation results for the main EPR spectra recorded at 100 K, and Figures S16 to S23 exhibit the corresponding spectra one by one, each time comparing the experimental spectrum to its simulated spectrum.

Table S24. Simulation results for the EPR spectra recorded at 100 K: EPR parameters given as g-values and A-values for each experimental spectrum.

	Details	Ratio (%)	Axial/iso	$g_{\|\|}$	$g_{\perp}$	$A_{\|\|}$ (MHz)	$A_{\perp}$ (MHz)	g_{iso}
$CuSO_4$	Complex 1	63	axial	2.344	2.095	450	0	-
	Complex 2	37	iso					2.155
$CuSO_4$+DMPO			axial	2.297	2.057	480	0	-
Cu-Phen			iso					2.115
Cu-Phen+DMPO			axial	2.287	2.061	466	0	-
$CuSO_4$+NaOH			axial	2.270	2.049	588	88	-
$CuSO_4$+ NaOH+DMPO	Poorly defined		axial	2.257	2.047	598	79.8	-
Cu-Phen+NaOH	Poorly defined		axial	2.268	2.049	592	88	-
Cu-Phen NaOH+DMPO			axial	2.250	2.048	593	87.4	-

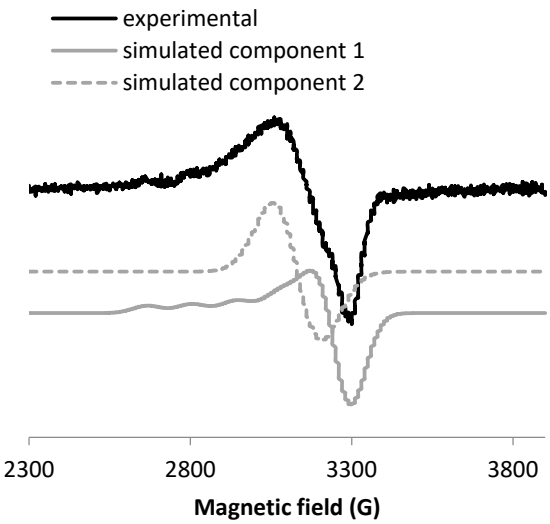

Figure S17. X-band EPR spectrum at 100 K of $CuSO_4$ and corresponding simulated spectrum

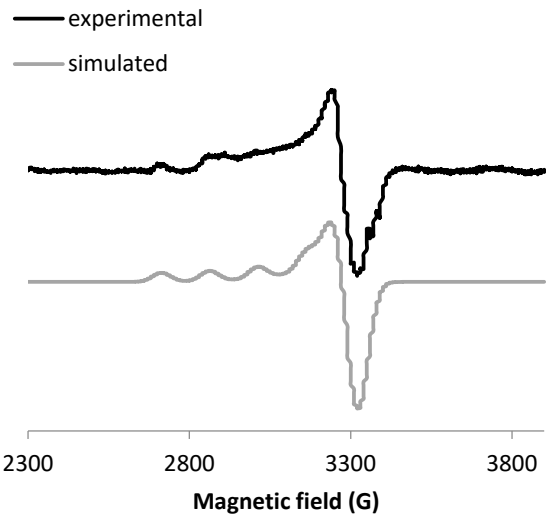

Figure S18. X-band EPR spectrum at 100 K of DMPO+$CuSO_4$ and corresponding simulated spectrum

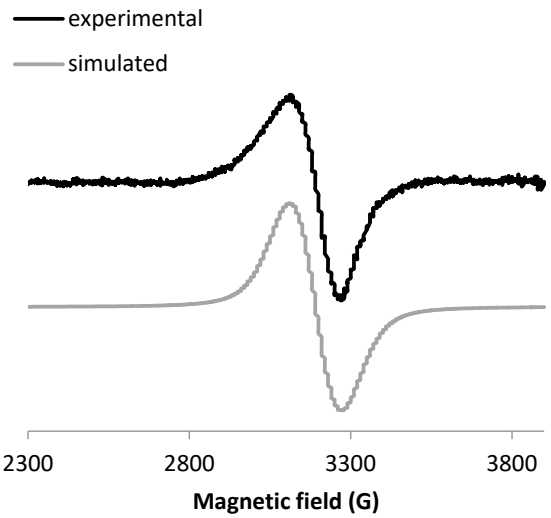

Figure S19. X-band EPR spectrum at 100 K of Cu-Phen and corresponding simulated spectrum

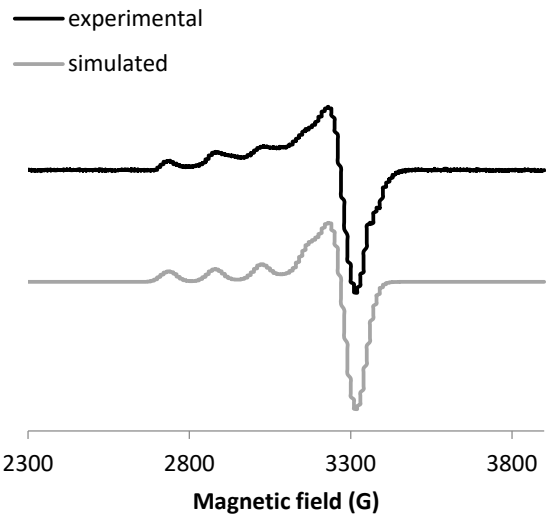

Figure S20. X-band EPR spectrum at 100 K of DMPO+Cu-Phen and corresponding simulated spectrum

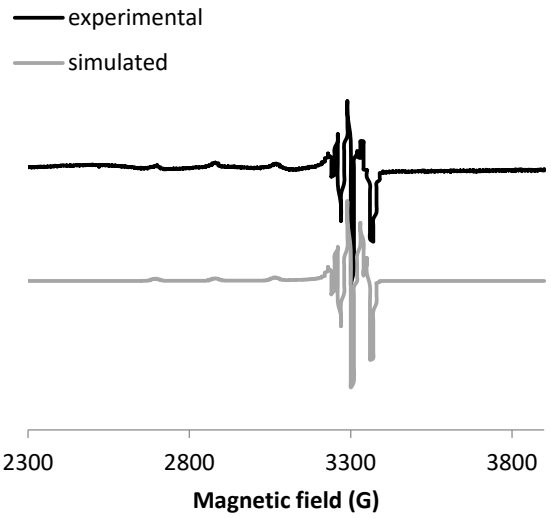

Figure S21. X-band EPR spectrum at 100 K of NaOH+$CuSO_4$ and corresponding simulated spectrum

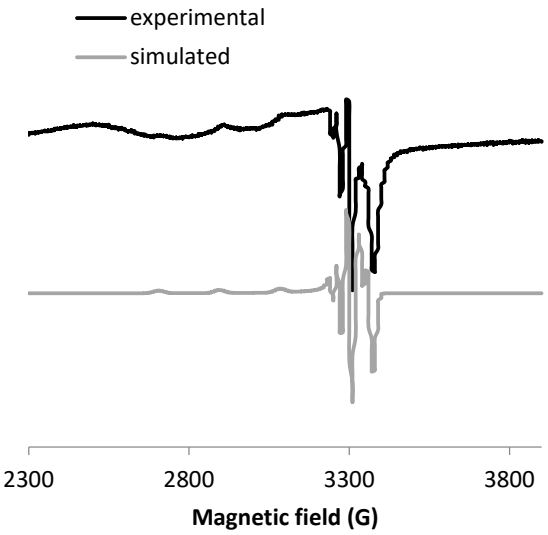

Figure S22. X-band EPR spectrum at 100 K of NaOH+DMPO+$CuSO_4$ and corresponding simulated spectrum

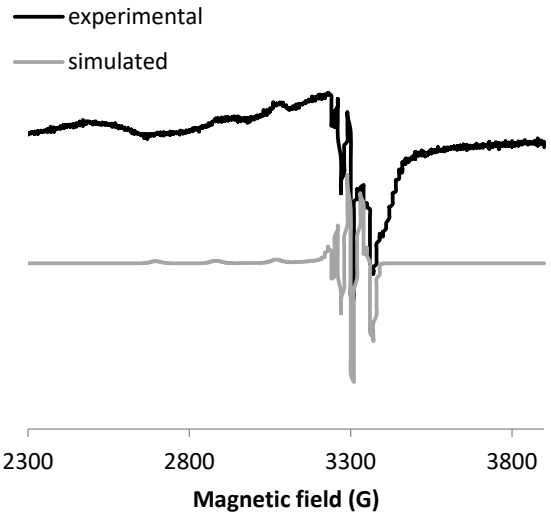

Figure S23. X-band EPR spectrum at 100 K of NaOH+ Cu-Phen and corresponding simulated spectrum

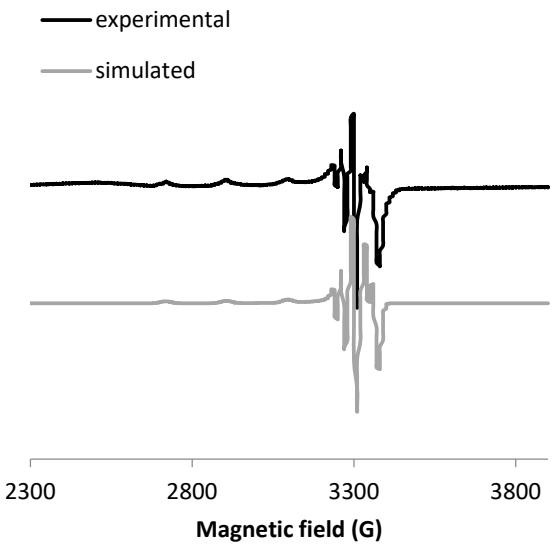

Figure S24. X-band EPR spectrum at 100 K of NaOH+DMPO+Cu-Phen and corresponding simulated spectrum